AADE-13-FTCE-21

Borehole Tortuosity Effect on Maximum Horizontal Drilling Length Based on Advanced Buckling Modeling

S.Menand, DrillScan US Inc.

Abstract

Borehole tortuosity is inherent to the rock drilling process and can be defined as the unwanted undulations from the planned well trajectory, such as borehole spiraling in vertical sections or slide-rotary pattern when using steerable mud motor in horizontal sections. It can sometimes compromise the success of the operation, especially in horizontal drilling, where additional drag can lead to problems while running completion strings.

Latest advancements in drill string mechanics have shown that borehole tortuosity (often ignored in standard buckling theories) plays a key role on the onset of buckling. The maximum horizontal length achievable by a given directional system (such as conventional rotary bottom hole assemblies, steerable mud motors and rotary steerable systems) depends not only on the severity of the borehole tortuosity along the horizontal section, but also on the build rate of the curve section. This paper shows the results of a sensitivity analysis using an advanced buckling model where different bore hole geometries have been studied.

Introduction

Tortuosity is recognized as a source of additional friction between tubular and borehole, responsible of casing and completions running difficulties, poor cementation and logging quality or casing wear issues. If many studies have been carried out in the past to quantify its effects on Torque & Drag, few have concerned the real impact of tortuosity on buckling onset. Having defined and discussed tortuosity and buckling (modeling, measurements, and field observations), this paper shows the effect of tortuosity on buckling onset. Eventually, this sensitivity analysis gives an estimation of the horizontal length lost due to excessive friction and buckling according to various tortuosity levels for 3 typical shale gas well trajectories.

Bore Hole Tortuosity

Introduction

Borehole tortuosity is inherent to the rock drilling process and can be defined as the unwanted undulations from the planned well trajectory. Tortuosity corresponds to borehole irregularities or oscillations, and can take many shapes, such as spiraling, rippling and hour-glassing[1,2,3,4,5,6]. Tortuosity is not only due to the directional drilling system steering or deviation principle, but can also be produced by some additional unwanted vibrations. It's worth noting also that the drilling bit itself has a strong influence on the tortuosity produced[7] (cutting structure and gage length). Rotary Steerable Systems (RSS), steerable mud motors (SM) and conventional rotary Bottom Hole Assemblies (BHA) do not produce the same level of tortuosity. RSS push-the-bit or point-the-bit systems (even with a closed loop system) activate and/or modify a steering force/pressure at a given frequency to push a pad or flex a shaft, to eventually reach a given directional objective or target. These frequent corrections produce tortuosity. However, it's generally accepted that the level of tortuosity generated by RSS is less important than a steerable mud motor. Indeed, the alternating of sliding and rotary phases of these latter systems generates a slide-rotary pattern. The magnitude of this tortuosity depends on many factors such as rock properties, drilling procedures, and wellbore geometry. Weijermans *et al*[1], by analyzing many wells drilled in North Sea by RSS or SM, estimated that the mean unwanted dog leg severity with RSS was about 0.54 deg./100ft in curve section and 0.41 deg./100ft in lateral/slant section. For SM, these figures were 0.79 deg./100ft in curve section and 0.46 deg./100ft in lateral/slant section.

Measurements

Surveys are taken generally every 30 or 90ft by Measurement While Drilling (MWD) tools and do not able to measure the actual tortuosity of the well bore on a smaller scale. Continuous MWD surveying has enabled to fill this gap by measuring inclination and azimuth every 30-90 seconds (every 1 to 3ft approximately), highlighting the tortuosity of the wellbore[3]. **Fig. 1** shows an example of standard and continuous surveys for a steerable mud motor, where the slide-rotary pattern is well recognized. Calipers, borehole imaging techniques and logging tools enable as well to detect and identify these borehole irregularities. Interestingly, it's worth mentioning some works about bending moment measurement in the BHA to estimate the dog leg severity, and thus the tortuosity[8] at a much higher resolution than standard surveys.

Modeling

During the planning phase, to better anticipate additional

friction between tubular and borehole, and calculate more realistic contact side forces, the current practice is to apply tortuosity over the planned survey in Torque & Drag model. This can be done by applying arbitrarily a mathematical function (generally sinusoidal or random variation of the inclination and azimuth over a given period length), which can be written generally as:

$$Inc._{tortuous} = Inc._{planned} + \Delta Inc.$$
$$Azi._{tortuous} = Azi._{planned} + \Delta Azi.$$

$Inc._{tortuous}$ and $Azi._{tortuous}$ correspond to the inclination and azimuth of the tortuous well path, by adding a given variation (ΔInc. and/or ΔAzi.) to the planned trajectory ($Inc._{planned}$ and $Azi._{planned}$). The two most important parameters in the tortuosity models are the amplitude and period of the variation. The amplitude corresponds to the maximum variation of angle applied over the planned survey (for example, from 0.1 to 1.5 deg.), and the period corresponds to the cycle length of the variation applied. Extreme attention should be taken to the period chosen to simulate the tortuosity. Indeed, a short period (typically 5-15 ft) will correspond to micro-tortuosity (such as borehole spiraling), although a longer period (typically 100-500 ft) will simulate preferably a slide-rotary pattern of a steerable mud motor (macro-tortuosity). For example, the period that could be chosen to simulate the slide-rotary pattern in **Fig. 1** is about 100 ft. **Fig. 2** shows a comparison between 3 distinct horizontal trajectories: a planned trajectory (perfectly smooth), a sinusoidal variation (period = 70ft amplitude = ± 1.2 deg.), a random variation (period = 6ft, amplitude = ± 0.5 deg. max) and an actual variation measured by a continuous survey measurement tool (period ≅ 80ft, amplitude ≅ ± 0.4 deg.).

It is highly recommended to plot and compare the inclination, azimuth and calculated dog leg severity of the simulated tortuous well path vs. the planned trajectory, to be sure that the mathematical variations entered in the model correspond well to the tortuosity desired.

In another way, recent studies[5,7] have shown that borehole tortuosity could be estimated using a BHA model coupled to a drill bit model to estimate inclination and azimuth in a step by step manner, every foot for example. The borehole tortuosity evaluation is much more realistic than mathematical models seen above, as they utilized the sliding or steering sheet of the directional system. The principle of this tortuosity evaluation is to perform a deflection analysis of the BHA at a given depth (given a tool-face orientation and operating parameters), and then predict inclination and azimuth for the next step (generally between 1 and 5ft) using a rock-bit interaction model, as explained in **Fig. 3**. The trajectory is then updated and incremented of this small step, and another calculation is then carried out. **Fig. 4** shows an actual case with an example of simulation produced with a steerable mud motor highlighting the slide-rotary pattern.

Whatever the tortuosity model taken into account (sinusoidal, random, BHA drill-ahead model), it's very important to choose a stiff-string torque and drag model with contact points capabilities to properly simulate the tortuosity effect on the drill string deformation. Indeed, if one assumes that the pipe curvature is equal to the wellbore curvature (as it is in soft-string torque and drag models, which assume no pipe stiffness and permanent low-side borehole contact), misleading results can be produced. Tubular is naturally stiff and does not follow the hole shape especially if the hole is tortuous and the clearance between pipe and borehole is important, as schematically shown in **Fig. 5**. Using a soft-string solution would mislead torque and drag results, as contact would be always located on the low side of the borehole whatever the tortuosity modeled (no stiffness and hole clearance effects).

Buckling

Introduction

Buckling occurs when the compressive load in a tubular exceeds a critical value, beyond which the tubular is no longer stable and deforms into a sinusoidal or helical shape (constrained buckling). It is worth noting that these two special shapes are a particular case for a given situation. Depending on the hole geometry, the shape of the buckled drill strings may take different forms. The sinusoidal buckling (first mode of buckling) corresponds to a tube that snaps into a sinusoidal shape and is sometimes called lateral buckling, snaking, or two-dimensional buckling. The helical buckling (second mode of buckling) corresponds to a tube that snaps into a helical shape (spiral shape). Lubinski initiated the first work dedicated to the buckling behavior of pipes in oil well operation. Since then, many theoretical works and/or experimental studies have been developed to better understand and model the buckling phenomenon and to take into account the effects due to wellbore geometry, dog leg severity, torque/torsion, tool-joint, friction, and rotation. The standard equation used to predict the occurrence of helical buckling in a straight and perfectly smooth deviated wellbore is given by:

$$F_{hel} = \lambda \sqrt{\frac{EI\omega \sin(Inc)}{r}} \quad \text{..... (Eq. 1)}$$

where EI is pipe stiffness, ω is the buoyed linear weight of the pipe, Inc is the wellbore inclination and r is the radial clearance between the pipe and the wellbore. The **λ** number varies from 2.83 to 5.65 depending on the author and on the different assumptions made. In conducting laboratory experiments and numerical analyses in a perfect horizontal well without rotation, Menand *et al*[9] and Thikonov *et al*[10] found similar results on the relationship between **λ** and the deformed shape of the drill pipes: **λ** close to 2.83 predicts the onset of the first helix, and **λ** close to 5.65 predicts the full helical drill string deformation in a perfect wellbore geometry

(without rotation).

However, recent studies have shown that the conventional buckling criteria (Eq. 1) are accurate only in perfect and idealized cases, but fail to predict buckling in a tortuous well bore, as dog legs play a great role on the buckling phenomenon. Using the standard and well-known buckling criteria may lead to conservative solutions. Indeed, drillstring or bottom hole assembly trips for buckling motivation are sometimes unjustified. Numerical modeling and laboratory tests have shown that drilling could continue safely even if the compressive load is greater than the conventional helical critical load[9,11,12,13]. It also has been shown that the axial force transfer remains good even though the pipe is helically buckled. Predicting accurately buckling in actual field conditions requires a numerical solution as the mechanical problem cannot be solved analytically or empirically. Most Torque & Drag & Buckling models are not realistic enough, as they do not correctly take into account the impact of tubular stiffness, hole clearance and tortuosity effects. The buckling model used in this paper has been fully validated with bench and field tests[11,12,13] and enables to overcome these modeling limitations.

Recently, a new Buckling Severity Index[11] has been proposed and focuses more on the bending stress level rather than shape taken by the pipe (sinusoidal or helical). Indeed, depending on the clearance between the pipe and the wellbore, bending stress in drill pipe created by dog legs is sometimes higher than bending stress produced by helical buckling. Consequently, helical buckling should not be always perceived as a dangerous situation. This new index, much more representative of the severity associated with buckling, is based on the bending stress (and its corresponding fatigue strength), the contact side force and the Von Mises stress, and ranges from 1 for a safe buckling condition with low risk of failure, to 4 for severe buckling with a high risk of failure or lock-up. Derivation of the Buckling Severity Index can be found in reference 11.

Modeling

Predicting accurately buckling in actual or simulated field conditions requires a numerical solution as the mechanical problem cannot be solved analytically or empirically. A numerical model dedicated to drillstring mechanics, from the drilling bit to the rig surface, has been developed to better predict and understand buckling in actual simulated conditions (originally developed in Mines ParisTech University[9]). More details, such as main hypotheses and resolution steps, can be found in reference 9.

This model has the ability to properly take into account the borehole tortuosity, even on a small scale (micro-tortuosity) as discretization of drill string and trajectory characteristics can be very accurate. Although the 3D mechanical behavior of drillstring is solved generally by using finite-element analysis, this model is based on a numerical solving of integral equations that reduces greatly the computational time. Any geometry of well trajectories can be simulated, with possible borehole enlargement, making this model very close to field conditions. The model includes a powerful contact algorithm based on an iterative process, and performs torque, drag, and buckling simultaneously, taking in account the friction analysis of the increased contact force generated by the buckling. These simultaneous Torque-Drag-Buckling calculations are run within a short iterative process to check the equilibrium state of the buckled drillstring.

Sensitivity Analysis

Methodology

A typical shale gas well architecture has been chosen for this sensitivity analysis, as shown in **Fig. 6**. Kick-off depth has been adjusted to keep constant the true vertical depth of the horizontal section (7000 ft), and build rates of the curve section and borehole tortuosity have been varied (build rate at 8, 12 and 16 deg./ 100ft) to estimate their effects on buckling. Characteristics of the 3 wells are presented in **Table 1**. It's worth mentioning that wells #2 and #3, thanks to the higher build rates in the curve section enable to reach the horizontal section at a lower measured depth and increase the reservoir exposure of 235 and 350ft respectively compared to the well#1. A $6^{1/8}$ in. BHA/drillstring has been chosen for this sensitivity analysis. The composition of the simplified BHA is as follows: PDC Bit, 100ft DC (ID=2 ¼ in., OD=4 ¾ in.), 935ft HWDP (ID=2 $^{9/16}$ in., OD=4 in. OD tool-joint=5 ¼ in.) and DP to surface (ID=3 $^{15/32}$ in., OD=4 in. OD tool-joint=5 ½ in.). Two operation types have been studied: running in hole (no rotation) and rotary drilling. Coefficient of friction between pipe and borehole is 0.2 (cased hole and open hole).

For each well (Wells #1, #2 and #3), planned and tortuous trajectories are compared in terms of buckling severity according to the level of tortuosity. Tortuosity has been added on planned trajectory only for the curve and lateral sections. The vertical section is assumed to be perfect (no tortuosity added). Four levels of tortuosity (Tort.#1, #2, #3 and #4) have been applied for each well trajectory as shown in **Table 2** and **Fig. 7**.

Results

Let's start by analyzing a buckling simulation result. **Fig. 8** shows an example of a running in hole simulation in the well#2 (with tortuosity Tort.#3 – see **Table 2**) at 17,500ft, showing that a buckling severity index of 4 has been reached in the curve section. **Fig. 9** shows the same simulation in terms of 3D deflection, contact side forces (red vectors) and bending moments. Many comments can be made from this result. Firstly, even though helical buckling is observed in the vertical section (see **Fig. 9)**, the buckling severity is medium/low (index=1 or 2) as bending stress and contact side forces are within an acceptable range (mean bending stress ≅ 5,000 psi and max contact side force ≅ 450 lbs), compared to the curve section where buckling severity is high (index=4).

Indeed, this section is characterized by high bending stress (up to 20,000 psi) and higher contact side forces (up to 1,800 lbs) even though drill pipes are not helically buckled. It's interesting to note numerous contact side forces outside the tool-joint section. Secondly, in the lateral section, moderate buckling is observed (index=2) with bending stresses up to 7,500 psi. At last, it's interesting to mention that the buckling shape follows the bottom and top of the sinusoidal variation added to the planned trajectory. Indeed, drill pipe contacts are on the low-side when the inclination is lower than 90 deg. and on the high-side when inclination is higher than 90 deg., following the period imposed by the tortuosity model (300ft in this example). Other results with different tortuosity periods suggest that buckled drill pipe shape is very dependent on the borehole tortuosity geometry.

Fig. 10 shows the tension/compression and associated buckling severity index along the drill string while running in hole the drill string at 17,500ft, for the 3 wells (no tortuosity, planned trajectory). If the 3 curves seem globally quite similar, differences in terms of buckling severity and drag friction can be observed in the curve section. Indeed, more drag friction is generated in the well #3 and a buckling severity index of 4 is reached on most part of the drill string localized in the curve. In order to quantify the effect of tortuosity on drag friction and buckling, similar simulations have been run in the 3 wells having different tortuosity levels. **Figs. 11** and **12** show the results of run in hole simulations for wells #2 and #3. One notices that tortuosity not only increases drag friction along the well trajectory (in the lateral and curve sections, as compression is higher), but also adds more stresses in the drill string since the buckling severity index 4 spreads along the curve section when tortuosity increases. Let's also notice that buckling severity index is mostly 4 for the well #3 regardless of the tortuosity level, due to the high average dog leg severity in the curve (16 deg. / 100ft).

All calculations have been run at a bit depth of 17,500ft, which corresponds to the maximum length achievable for the well#2 in run in hole operation for this set of parameters. Indeed, buckling severity index reaches a value of 4, which could jeopardize the success of the operation.

To estimate and compare the horizontal length lost due to friction in the curve and due to tortuosity for the 3 wells, one has applied the following methodology. Drag friction for each well is calculated in the curve (drag friction per 100ft) as shown in **Fig. 12** and **Table 3**. In this example, drag is equal to 8.1 klbs over the 554ft of the curve, which is equivalent to a drag of 1.46 klbs/100ft (well#3, Tort.#3). In comparing all the results (see **Table 3**), one notices for example that drag friction is 4 to 5 times higher in well#3 than in well#1 due to higher contact side forces in the curve. In shale gas wells, most of the drag friction is lost in the lateral section which can be as long as 10,000 ft. This drag friction determines generally the maximum horizontal length that can be achieved before lock-up or severe buckling (too much compression in the drill string). This drag friction has also been calculated in the lateral section as a function of tortuosity level (see **Table 3**). As one could expect, higher drag friction is produced with higher tortuosity. In comparing drag friction generated in the curve with one generated in the lateral section, one can try to evaluate the horizontal length lost due to drag friction in the curve (see **Table 4**). Eventually, the aim is to know which of the 3 wells enables to maximize the horizontal length. **Table 4** shows that equivalent length losses of well#2 and well#3 are respectively and approximately 200ft and 400ft more important than well#1. Remembering that wells#2 and #3 have a longer reservoir exposure than well#1 (respectively 235 and 350ft), one can conclude that the well#2 enables to maximize the horizontal length for this case studied.

Figs. 13 and **14** show the results of simulation for the rotary mode at 17,500ft (a weight on bit of 20 klbs and torque on bit of 3500 lbf.ft have been assumed) for the 3 wells and all tortuosity levels. As friction is lost entirely in torque, tortuosity and build rate have logically no effect on the tension/compression, and all curves overlap. However, a buckling severity index of 3 is reached in the curve section, and sinusoidal buckling is observed along the lateral section with a buckling severity index of 2 (see **Fig. 15**). **Fig. 14** shows that torque increases with increasing tortuosity level (about 10 % between planned and tortuosity Tort. #4 for these cases studied). No significant difference is observed between each well given a tortuosity level.

Conclusions

Borehole tortuosity is inherent to the rock drilling process and can sometimes compromise the success of the drilling or completion operations. Borehole tortuosity effect on buckling has been studied in considering 3 typical shale gas well architectures, and the following conclusions can be derived:

- Borehole tortuosity geometry influences strongly the shape taken by the buckled tubular. As tubular is constrained within the tortuous wellbore, it has a tendency to follow the geometry imposed by the hole.
- Borehole tortuosity not only adds friction between the tubular and the borehole, but also eases the onset of buckling compared to a smooth borehole
- The build rate of the curve has a strong influence on the buckling severity and can produce strong contact side forces and bending moment if rate is higher than 16 deg./100ft.
- Buckling severity index enables to better quantify the severity of buckling compared to the standard helical buckling criterion which can occasionally be safely exceeded.

Nomenclature

BHA = *Bottom Hole Assembly*
RSS = *Rotary Steerable System*
SM = *Steerable Motor*
MWD = *Measurement While Drilling*
Inc. = *Inclination (deg.)*
Azi. = *Azimuth (deg.)*

E = *Young's Modulus, Pa*
F = *Compressive Load, N*
F_{hel} = *Helical critical compressive force, N*
I = *Moment of inertia of drill pipes, m4*
r = *Radial clearance, m*
ω = *Buoyed linear weight of drill pipe, N/m*
λ = *Constant, no unit*

References

1. Weijermans, P., Ruszka J., Jamshidian H., Matheson M.: "Drilling with Rotary Steerable System Reduces Wellbore Tortuosity", paper SPE/IADC 67715, SPE/IADC Drilling Conference held in Amsterdam, The Netherlands, 27 February–1 March 2001
2. Brands S., Lowdon R.: "Scaled Tortuosity Index:Quantification of Borehole Undulations in terms of Hole Curvature, Clearance and Pipe Stiffness", paper SPE/IADC 151274, SPE/IADC Drilling Conference held in San Diego, California, USA, 6-8 March 2012
3. Stockhausen E.J. and Lesso W.G. Jr : "Continuous Direction and Inclination Measurements Lead to an Improvement in Wellbore Positioning", paper SPE/IADC 79917, presented at the SPE/IADC Drilling Conference held in Amsterdam, The Netherlands 19-21 February 2003.
4. Gaynor T.M., Chen D.C-K., Stuart D., Comeaux B.: Tortuosity versus Micro-Tortuosity – Why Little Things Mean a Lot", paper SPE/IADC 67818, SPE/IADC Drilling Conference held in Amsterdam, The Netherlands, 27 February–1 March 2001
5. Pastusek P., Brackin V.: "A model for Borehole Oscillations", paper SPE/IADC 84448, SPE Annual Technical Conference and Exhibition held in Denver, Colorado, USA, 5-8 October 2003
6. Samuel G.R. and Bharucha K. : "Tortuosity Factors for Highly Tortuous Wells : A practical Approach", paper SPE/IADC 92565 presented at the SPE/IADC Drilling Conference held in Amsterdam, The Netherlands, 23-25 February 2005
7. Menand S., Simon C., Gaombalet J., Macresy L., Gerbaud L., Ben Hamida M., Amghar Y., Denoix H., Cuiller B., Sinardet H. : "PDC Bit Steerability Modeling and Testing for Push-the-bit and Point-the-bit RSS", paper SPE 151283, IADC/SPE Drilling Conference, 6-8 March 2012, San Diego, CA, USA
8. Heisig G., Cavallaro G., Jogi P., Hood J. and Forstner I. : "Continuous Borehole Curvature Estimates While Drilling Based on Downhole Bending Moment Measurements", paper SPE 90794, presented at the SPE Annual Technical Conference and Exhibition held in Houston, Texas, USA, 26-29 September 2004
9. Menand S., Sellami H., Tijani M. and Akowanou J. : "Buckling of Tubulars in Actual Field Conditions", paper SPE102850, presented at the 2006 SPE Annual Technical Conference and Exhibition, 24-27 September 2006, San Antonio, Texas, USA
10. Tikhonov V.S., Safronov A.I. and Gelfat M.Y. "Method of Dynamic Analysis of Rod-In-Hole Buckling", ESDA2006-95059, Proceedings of ESDA 2006. 8th Biennal ASME Conference on Engineering Systems Design and Analysis, July 4-7, Torino, Italy
11. Menand S. "A New Buckling Severity Index to Quantify Failure and Lock-up Risks in Highly Deviated Wells", paper SPE 151279, 2012 SPE Deepwater Drilling and Completions Conference and Exhibition, 20 - 21 June 2012, Galveston, Texas, USA
12. Menand S., Bjorset A., Macresy L.: , "A New Buckling Model Successfully Validated with Full-Scale Buckling Tests", AADE 2011 National Technical Conference & Exhibition, April 12-14, 2011 at the Hilton Houston North Hotel in Houston, Texas
13. Menand S., Chen D. "Safely Exceeding Buckling Loads in Long Horizontal Wells: Case Study in Shale Plays", paper SPE 163518, 2013 IADC/SPE Drilling Conference, Amsterdam, The Netherlands

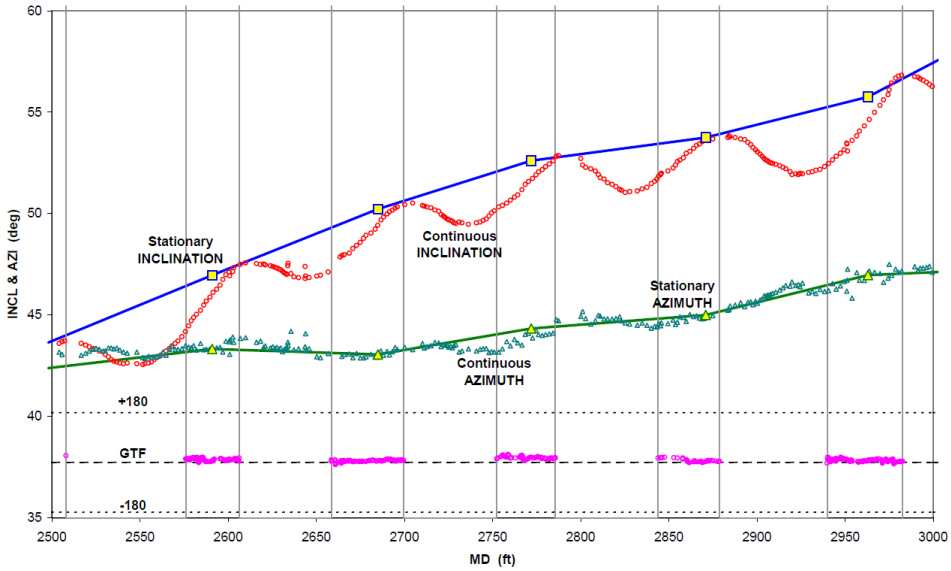

Figure 1: Typical Slide-Rotary pattern of a steerable mud motor (Source: Stockhausen *et al*[3])

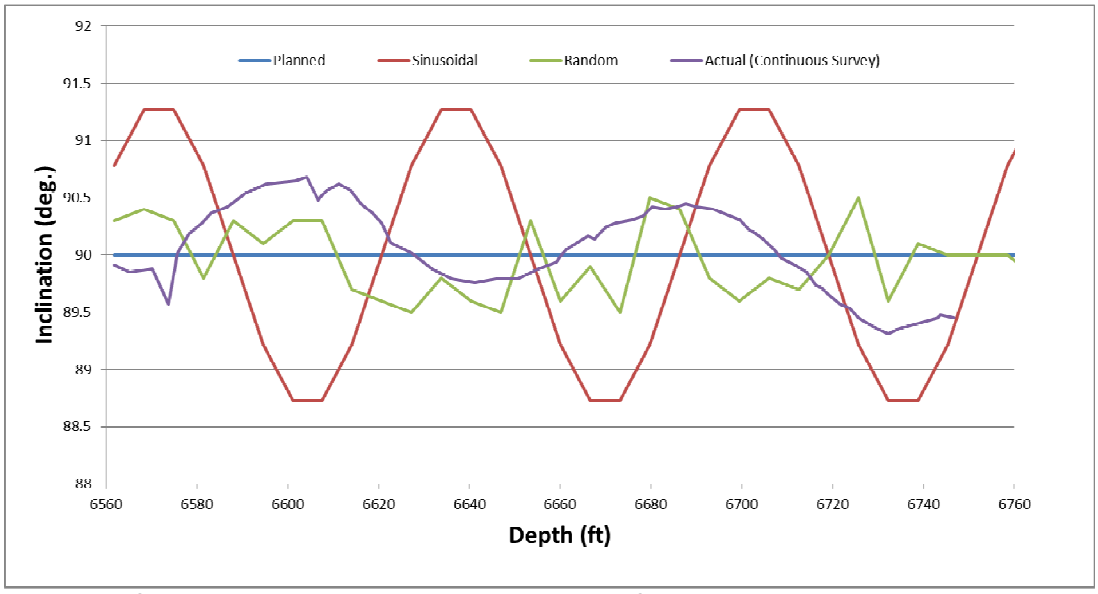

Figure 2: Example of borehole tortuosity. Planned trajectory (perfectly smooth), Sinusoidal variation (period = 70ft, amplitude = ± 1.2 deg.), Random variation (period = 6ft, amplitude = ± 0.5 deg. max) and an actual variation measured by a continuous survey measurement tool (period ≅ 80ft, amplitude ≅ ± 0.4 deg.).

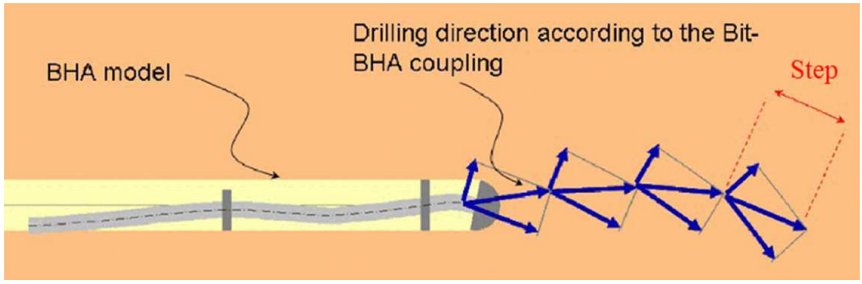

Figure 3: Tortuosity estimation with a rock-bit model coupled to BHA model

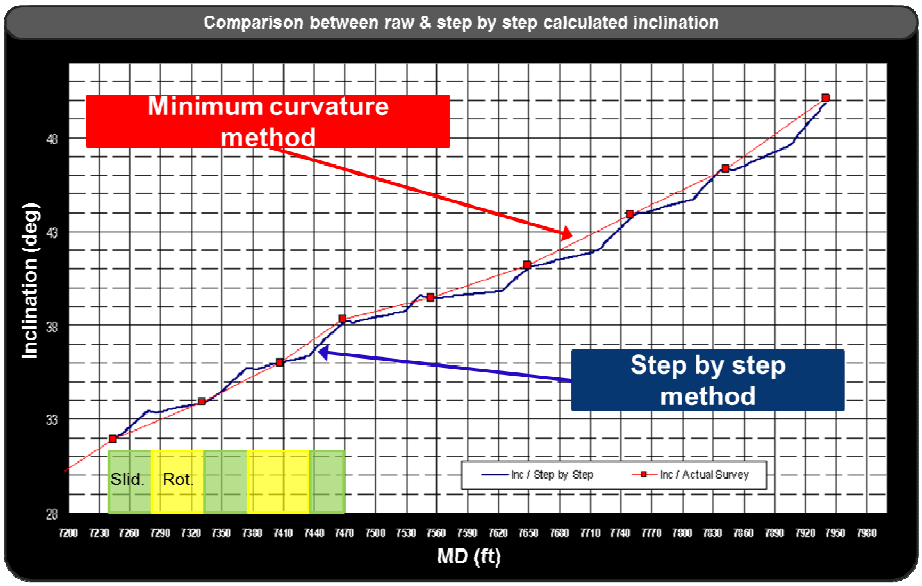

Figure 4: Calculated Slide-Rotary pattern using a rock-bit model coupled to BHA model

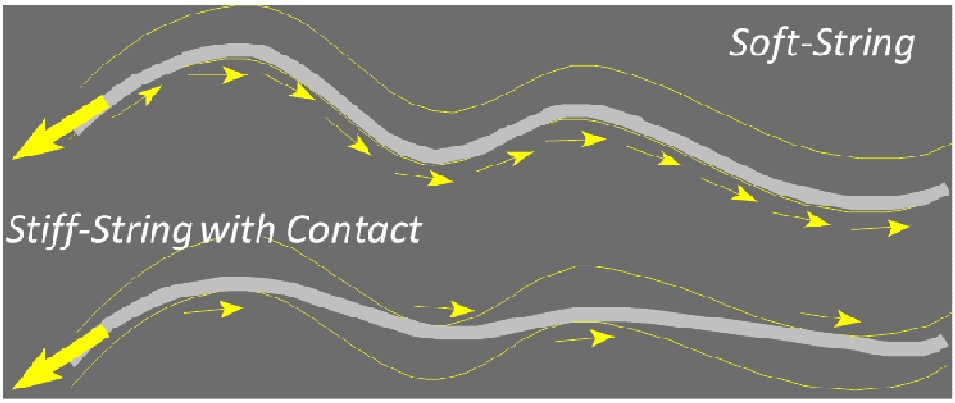

Figure 5: Schematics illustrating modeling difference between Soft-string and Stiff-string model in presence of tortuosity

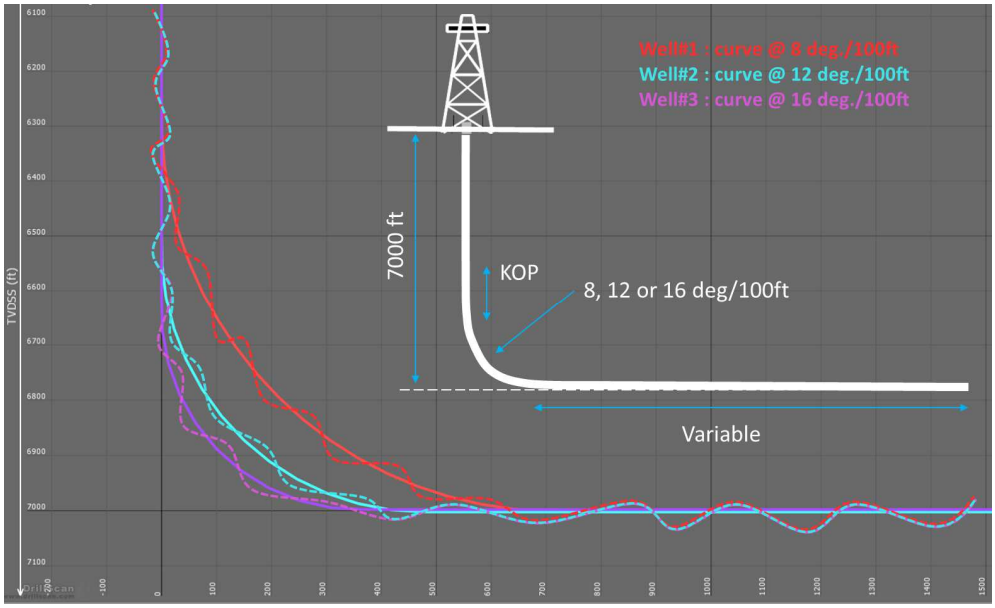

Figure 6: Shale Gas Well trajectories

Table 1: Well Trajectories

Parameters	Well#1	Well#2	Well#3
Mean Build Rate In the Curve (deg./100 ft)	8	12	16
Kick Off point (ft)	6284	6522	6642
Horizontal Section TVD (ft)	7000	7000	7000
Gain in reservoir exposure compared to Well #1 (ft)	0	235	350
Hole Size (in.)	6 1/8	6 1/8	6 1/8
Mud Weight (ppg)	9.50	9.50	9.50
7" Casing Shoe depth (ft)	7420	7280	7210

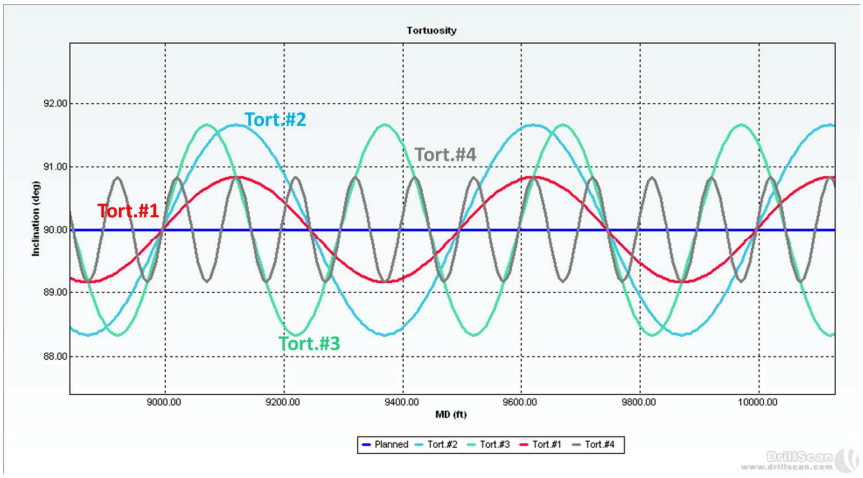

Figure 7: Simulated Tortuosity – Variation of inclination in the lateral section

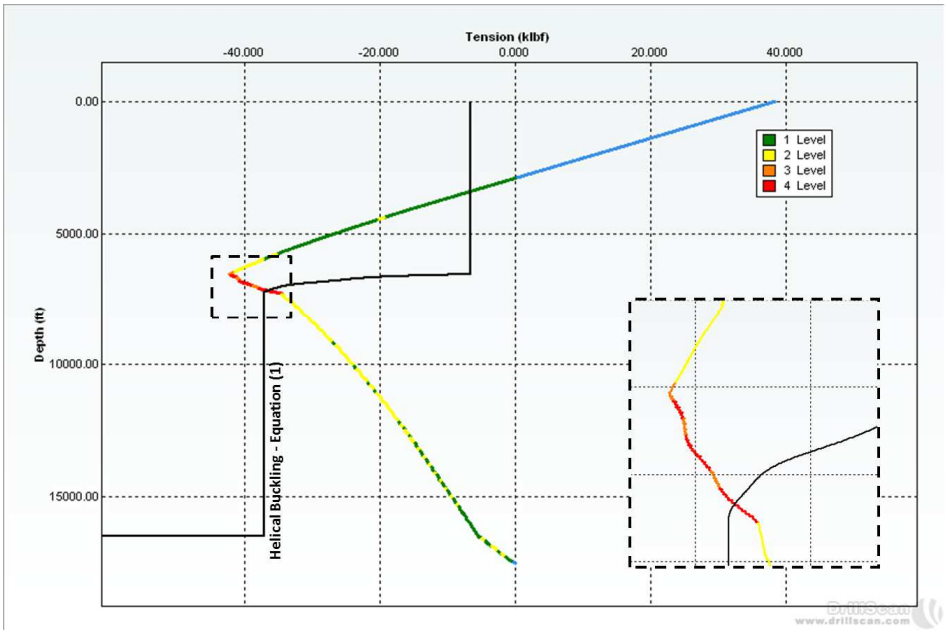

Figure 8: Well#2 – Tortuosity Tort.#3 – Tension/compression along the drillstring while running in hole @17,500ft - Buckling Severity Index

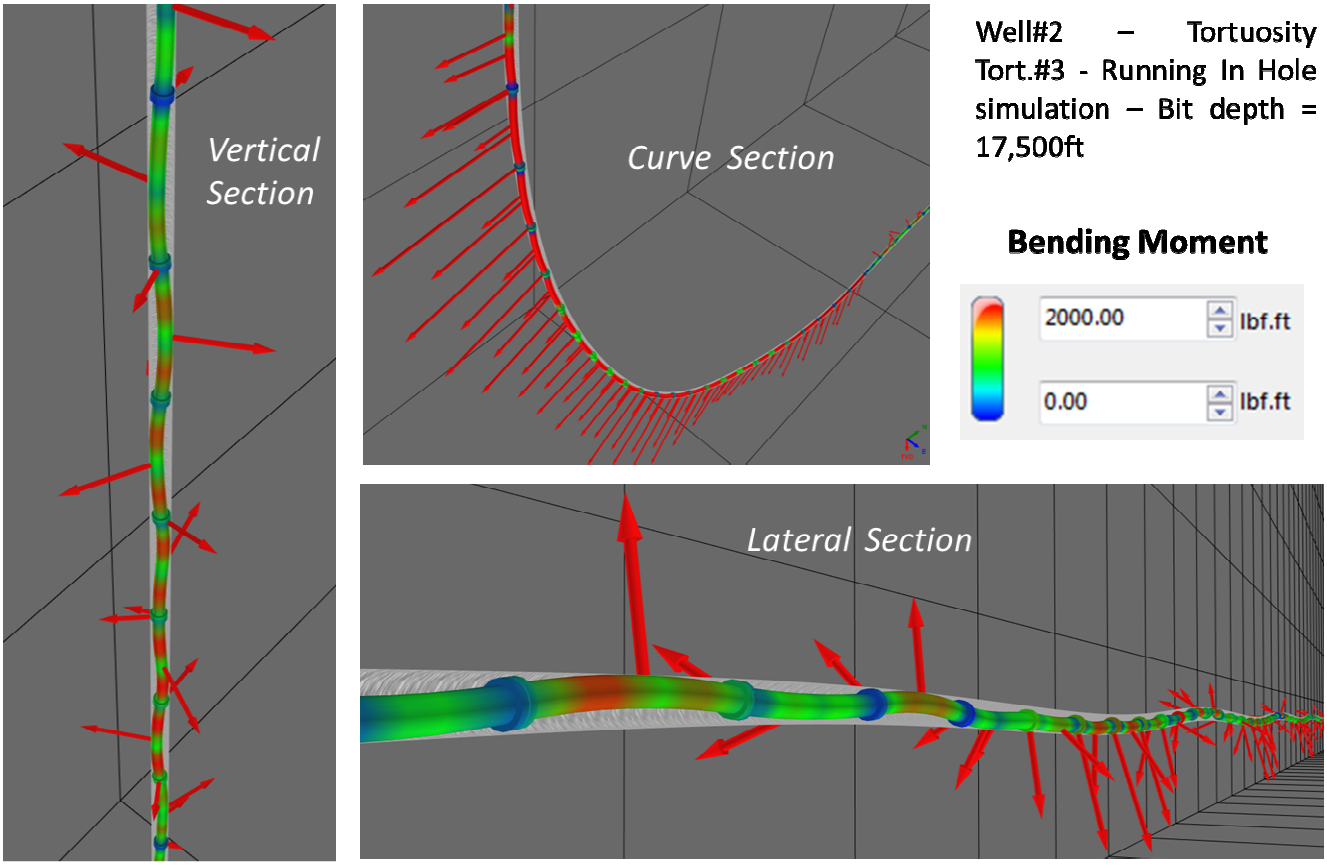

Figure 9: 3D deflection, Contact Side Force and Bending Moment while running in hole @17,500ft

Table 2: Tortuosity parameters

Parameters	Tort.#1	Tort.#2	Tort.#3	Tort.#4
Tortuosity Type	Sinusoidal	Sinusoidal	Sinusoidal	Sinusoidal
Period (ft)	500	500	300	100
Max Variation Inc.	0.83 deg.	1.67 deg.	1.67 deg.	0.83 deg.
Max Variation Azi.	0.42 deg.	0.83 deg.	0.83 deg.	0.42 deg.
Mean Dog Leg Severity in lateral section (deg. / 100ft)	0.75	1.49	2.48	3.80

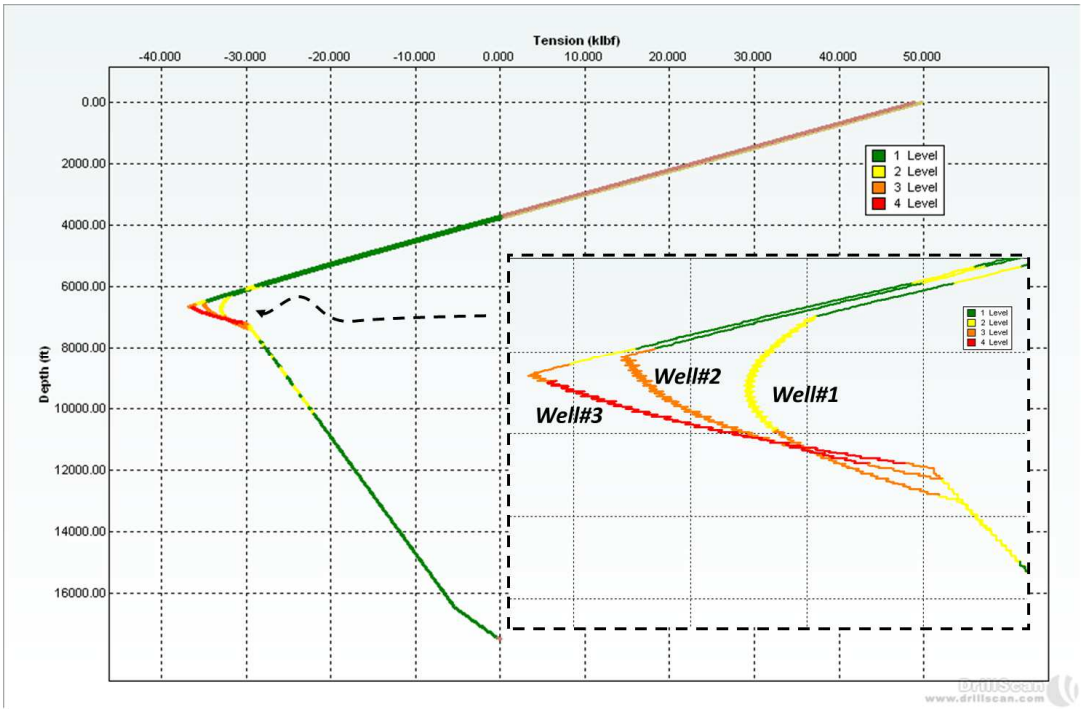

Figure 10: Tension/compression along the drillstring while running in hole @17,500ft - Buckling Severity Index – Wells #1, #2, #3 – Planned wells

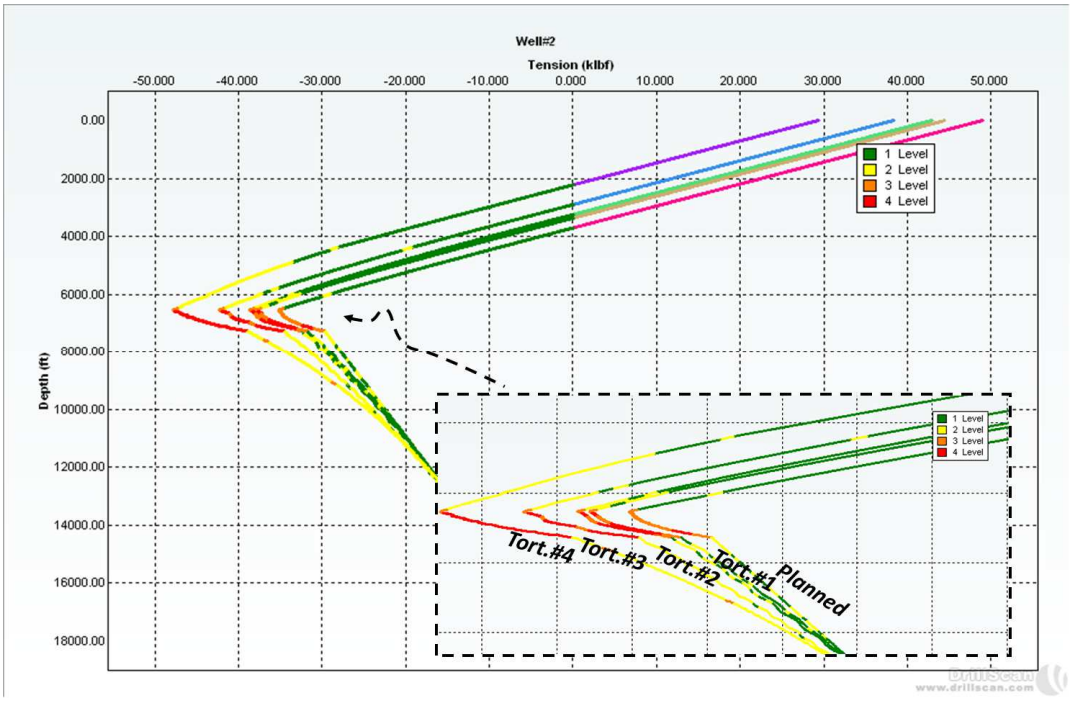

Figure 11: Tension/compression along the drillstring while running in hole @17,500ft - Buckling Severity Index – Wells #2 (Planned and different Tortuosity Levels)

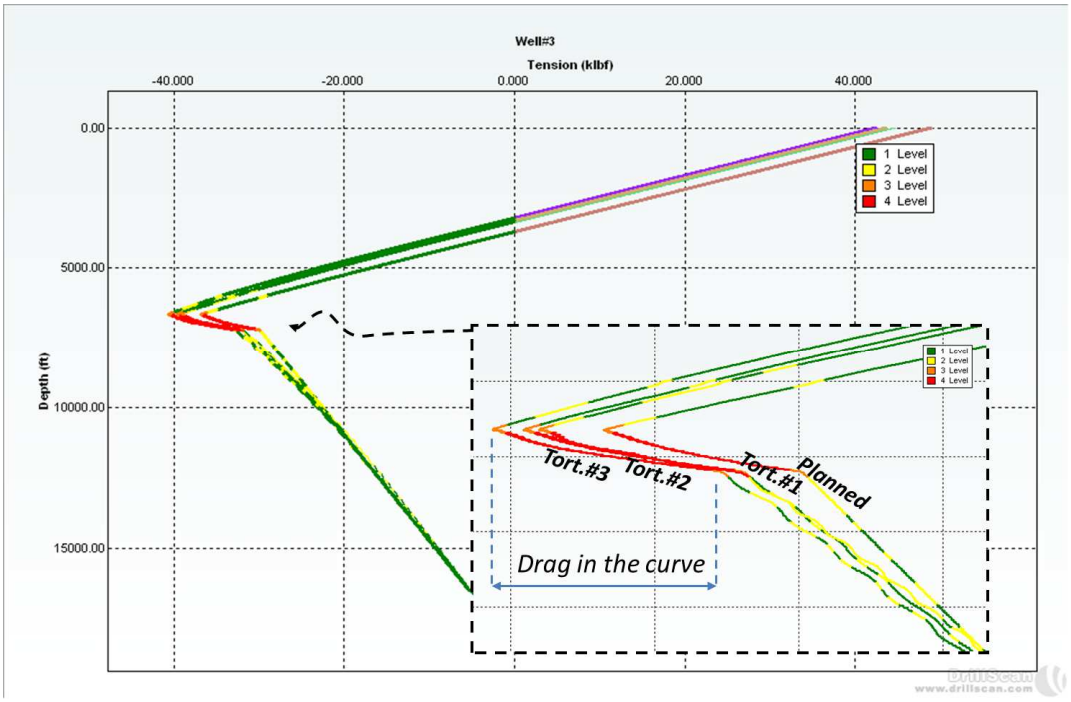

Figure 12: Tension/compression along the drillstring while running in hole @17,500ft - Buckling Severity Index – Wells #3 (Planned and different Tortuosity Levels)

Table 3: Drag friction while running in hole at 17,500ft

	Planned	Tort.#1	Tort.#2	Tort.#3	Tort.#4
Drag friction in the curve section (klbs/ 100 ft)					
Well#1	0.19	0.27	0.33	0.41	0.61
Well#2	0.70	0.83	0.87	1.03	1.21
Well#3	1.28	1.34	1.37	1.46	*Elastic limits exceeded*
Drag friction in the lateral section (klbs/100 ft)					
Wells #1,#2,#3	0.26	0.28	0.29	0.31	0.36

Table 4: Equivalent length lost in lateral section

	Planned	Tort.#1	Tort.#2	Tort.#3	Tort.#4
Equivalent Length Lost in Lateral Section due to Drag in the Curve					
Well#1 (ft)	73	96	114	131	172
Well#2 (ft)	271	294	304	331	337
Well#3 (ft)	493	475	481	470	*Elastic limits exceeded*

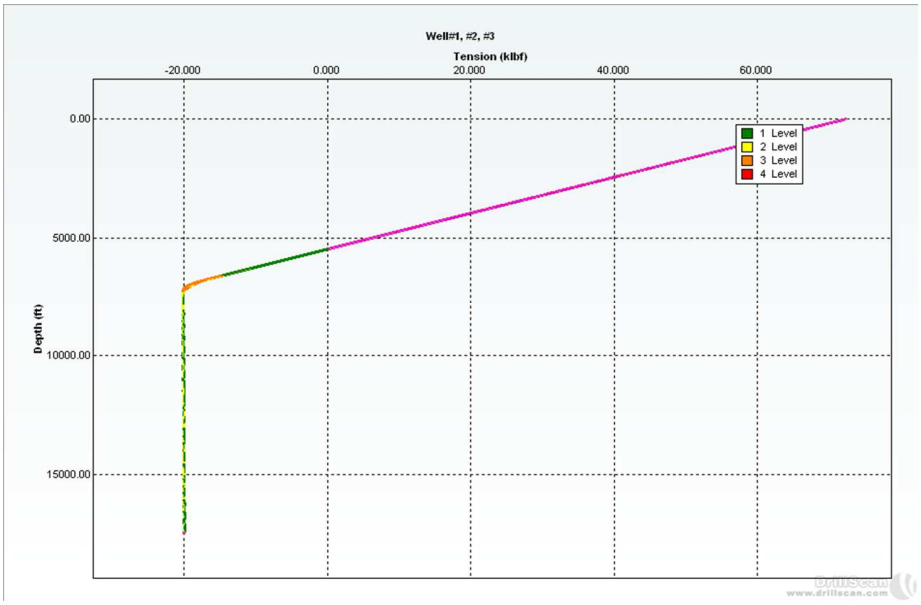

Figure 13: Tension/compression along the drillstring while drilling in rotary @ 17,500ft - Buckling Severity Index – Wells #1, #2, #3 (Planned and different Tortuosity Levels)

Figure 14: Torque along the drillstring while drilling in rotary mode @ 17,500ft - Wells #1, #2, #3 (Planned and different Tortuosity Levels)

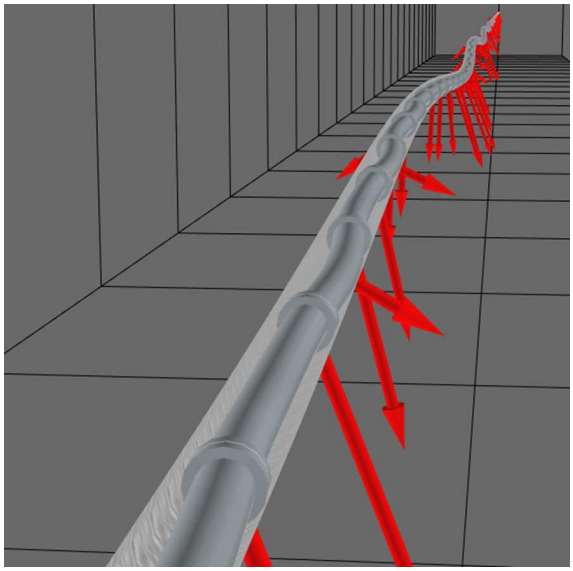

Figure 15: Sinusoidal buckling observed while drilling at 17,500ft (WOB=20 klbs, TOB=3,500 lbf.ft) – Wells#1, #2, #3 – Tortuosity #2